

Classical and semiclassical investigations of models for real scalar fields

D. Bazeia, A. S. Inácio, and L. Losano
Departamento de Física, Universidade Federal da Paraíba
Caixa Postal 5008, 58051-970 João Pessoa, Paraíba, Brazil
 (February 12, 2019)

We investigate several models described by real scalar fields, searching for topological defects, and investigating their linear stability. We also find bosonic zero modes and examine the thermal corrections at the one-loop level. The classical investigations may be of interest to high energy physics and applications to nonlinear science. The semiclassical investigations show that the finite temperature corrections that appear in a specific model do not suffice to fully restore the symmetry at high temperature.

PACS numbers: 11.10.Lm, 11.27.+d

I. INTRODUCTION

Models described by real scalar fields in $(1,1)$ space-time dimensions are among the simplest systems that support topological solutions. Usually, these topological solutions are named kinks, which are classical static solutions of the equations of motion, and the topological behavior is related to the asymptotic form of the field configurations, which has to differ in both the positive and negative space directions. To ensure that the classical solutions have finite energy, one requires that the asymptotic behavior of the solutions is identified with minima of the potential that defines the system under consideration, so in general the potential has to include at least two distinct minima in order for the system to support topological solutions.

We can investigate real scalar fields in $(3,1)$ space-time dimensions, and now the topological solutions are named domain walls. These domain walls are bidimensional structures that carry surface tension, which is identified with the energy of the classical solutions that spring in $(1,1)$ space-time dimensions. The domain wall structures are supposed to play a role in applications to several different contexts, ranging from the low energy scale of condensed matter [1–3] up to the high energy scale required in the physics of elementary particles, fields and cosmology [4–6].

There are at least three classes of models that support kinks or domain walls, and we further explore such models in the next Sec. II. In the first class of models one deals with a single real scalar field, and the topological solutions are structureless. Examples of this are the sine-Gordon and ϕ^4 models [4]. In the second class of models one also deals with a single real scalar field, but now the systems comprise at least two distinct domain walls. An example of this is the double sine-Gordon model, which has been investigated for instance in Refs. [7–10]. In the third class of models we deal with systems defined by two real scalar fields, and now one opens two new possibilities: domain walls that admit internal structure [11–17], and junctions of domain walls, which appear in models of two

fields when the potential contains non-colinear minima, as recently investigated for instance in Refs. [18–30].

There are other motivations to investigate domain walls in models of field theory, one of them being related to the fact that the low energy world volume dynamics of branes in string and M theory may be described by standard models in field theory [31–33]. Besides, one knows that field theory models of scalar fields may also be used to investigate properties of quasi-linear polymeric chains, as for instance in the applications of Refs. [34–37], to describe solitary waves in ferroelectric crystals, the presence of twistons in polyethylene, and solitons in Langmuir films.

In the present work, in Sec. II we review some known facts on kinks and domain walls, and there we also introduce other results. In particular, we present some new models described by one and by two real scalar fields. The investigations follow in Sec. III where we search for the topological structures that generate kinks and walls. We reserve for Sec. IV the study of stability of the solutions that we found in the former section. We investigate the finite temperature effects in Sec. V, where we examine the effective potential for a specific model, which engenders three minima at the classical level. We end the work in Sec. VI, where we comment on applications to nonlinear science and briefly review the results of the present investigation.

II. GENERAL CONSIDERATIONS

In this work we are interested in field theory models that describe real scalar fields and support topological solutions of the Bogomol’nyi-Prasad-Sommerfield (BPS) type [38,39]. In the case of a single real scalar field ϕ , we consider the Lagrange density

$$\mathcal{L} = \frac{1}{2} \partial_\alpha \phi \partial^\alpha \phi - V(\phi) \quad (1)$$

Here $V(\phi)$ is the potential, which identifies the particular model under consideration. We write the potential

in the form $V(\phi) = (1/2)W_\phi^2$, where $W = W(\phi)$ is a smooth function of the field ϕ , and $W_\phi = dW/d\phi$. In a supersymmetric theory W is the superpotential, and this is the way we name W in this work.

The equation of motion for $\phi = \phi(x, t)$ has the general form

$$\frac{\partial^2 \phi}{\partial t^2} - \frac{\partial^2 \phi}{\partial x^2} + \frac{dV}{d\phi} = 0 \quad (2)$$

and for static solutions we get

$$\frac{d^2 \phi}{dx^2} = W_\phi W_{\phi\phi} \quad (3)$$

It was recently shown in Refs. [40,41] that this equation of motion is equivalent to the first order equations

$$\frac{d\phi}{dx} = \pm W_\phi \quad (4)$$

if one is searching for solutions that obey the boundary conditions $\lim_{x \rightarrow -\infty} \phi(x) = \bar{\phi}_i$ and $\lim_{x \rightarrow -\infty} (d\phi/dx) = 0$, where $\bar{\phi}_i$ is one among the several vacua $\{\bar{\phi}_1, \bar{\phi}_2, \dots\}$ of the system. In this case the topological solutions are BPS (+) and anti-BPS (-) solutions. Their energies get minimized to the value $t^{ij} = |\Delta W_{ij}|$, where $\Delta W_{ij} = W_i - W_j$, with W_i standing for $W(\bar{\phi}_i)$. The BPS and anti-BPS solutions are defined by two vacuum states belonging to the set of minima that identify the several topological sectors of the model.

In the case of two real scalar fields ϕ and χ the potential is written in terms of the superpotential, in a way such that $V(\phi, \chi) = (1/2)W_\phi^2 + (1/2)W_\chi^2$. The equations of motion for static fields are

$$\frac{d^2 \phi}{dx^2} = W_\phi W_{\phi\phi} + W_\chi W_{\chi\phi} \quad (5)$$

$$\frac{d^2 \chi}{dx^2} = W_\phi W_{\phi\chi} + W_\chi W_{\chi\chi} \quad (6)$$

which are solved by the first order equations

$$\frac{d\phi}{dx} = W_\phi \quad \frac{d\chi}{dx} = W_\chi \quad (7)$$

or

$$\frac{d\phi}{dx} = -W_\phi \quad \frac{d\chi}{dx} = -W_\chi \quad (8)$$

Solutions to these first order equations are BPS (+) and anti-BPS (-) states. They solve the equations of motion, and have energy minimized to $t^{ij} = |\Delta W^{ij}|$ as in the case of a single field; here, however, $\Delta W^{ij} = W(\phi_i, \chi_i) - W(\phi_j, \chi_j)$, since now we need a pair of numbers (ϕ_i, χ_i) to represent each one of the vacuum states in the system of two fields. In the plane (ϕ, χ) we may have minima that are non colinear, opening the possibility for junctions of defects. In the case of two real

scalar fields, we can find a family of first order equations that are equivalent to the pair of second order equations of motion, but this requires that $W_{\phi\phi} + W_{\chi\chi} = 0$, in the case of harmonic superpotentials [40,41].

We now turn attention to kinks and domain walls. Perhaps the most known example of this is given by the ϕ^4 model, defined by the potential $V(\phi) = (1/2)(\phi^2 - 1)^2$. Here we are using natural units, and dimensionless fields and coordinates. In this model the domain wall can be represented by the solution $\phi_s(x) = \pm \tanh(x)$. The above potential can be written with the superpotential $W(\phi) = \phi - \phi^3/3$, and the domain wall is of the BPS or anti-BPS type. The wall tension corresponding to the BPS wall is $t_s = 4/3$.

We can also find structureless domain walls in other models, for instance in the ϕ^6 model, which is described by the potential $V(\phi) = (1/2)\phi^2(\phi^2 - 1)^2$. Here we have $W(\phi) = (1/2)\phi^2 - (1/4)\phi^4$, and the wall configurations are also of the BPS type, and are given by $\bar{\phi}_s^2 = (1/2)[1 \pm \tanh(x)]$. The wall tension is now $t_s = 1/4$. This potential was investigated for instance in Ref. [42].

We can build at least two other classes of models where the domain walls engender other features. The next class is yet described by a single field, but the systems may now support two or more different walls. An interesting example of this is the double sine-Gordon model, which is defined by the potential

$$V_r(\phi) = \frac{1}{r+1} [4r \cos(\phi) + \cos(2\phi)] \quad (9)$$

where r is a parameter, real and positive. This potential is periodic, with period 2π ; for simplicity in the following we consider the interval $-2\pi < \phi < 2\pi$. The value $r = 1$ distinguishes two regions, the region $r \in (0, 1)$ where the potential contains four minima, and the region $r \geq 1$, where the potential contains two minima. For $r \in (0, 1)$ the system supports two distinct wall configurations, the large wall and the small wall, which distinguish the two different barrier the model comprises in this case. The limits $r \rightarrow 0$ and $r \rightarrow \infty$ lead us back to the sine-Gordon model. The double sine-Gordon model has been considered in several distinct applications, as for instance in Ref. [7–10], where one investigates magnetic solitons in superfluid ^3He , kink propagation in a model for poling in polyvinylidene fluoride, and properties related to the two different kinks that appear in such polymeric chain.

To expose new features of the double sine-Gordon model we rewrite Eq. (9) in the form

$$V_r(\phi) = \frac{2}{1+r} [\cos(\phi) + r]^2 \quad (10)$$

where we have omitted an unimportant r -dependent constant. The model can be described by the superpotential

$$W(\phi) = \frac{2}{\sqrt{1+r}} [\sin(\phi) + r\phi] \quad (11)$$

For r in the interval $r \in (0, 1)$ the minima of the potential are the singular points of the superpotential, $dW/d\phi = 0$.

They are periodic, and for $-2\pi < \phi < 2\pi$ there are four minima, at the points $\bar{\phi} = \pm\pi \pm \alpha(r)$, where $\alpha(r) = \cos^{-1}(r)$. For $r \geq 1$ the minima are at $\bar{\phi} = \pm\pi$, in the interval $-2\pi < \phi < 2\pi$. A closer inspection shows that for $0 < r < 1$ the local maxima at $\pm\pi$ and the minima $\pm\pi \pm \alpha(r)$ degenerate to the minima $\pm\pi$ for $r = 1$, and remain there for $r > 1$. Thus, the parameter r induces a transition in the behavior of the double sine-Gordon model. The value $r = 1$ is the critical value, since it is the point where the system changes behavior: for $r \in (0, 1)$ this model supports minima that disappear for $r \geq 1$. We illustrate the double sine-Gordon model in Fig. 1, where we depict the potential of Eq. (10) for $r = 1/3, 2/3$ and for $r = 1$.

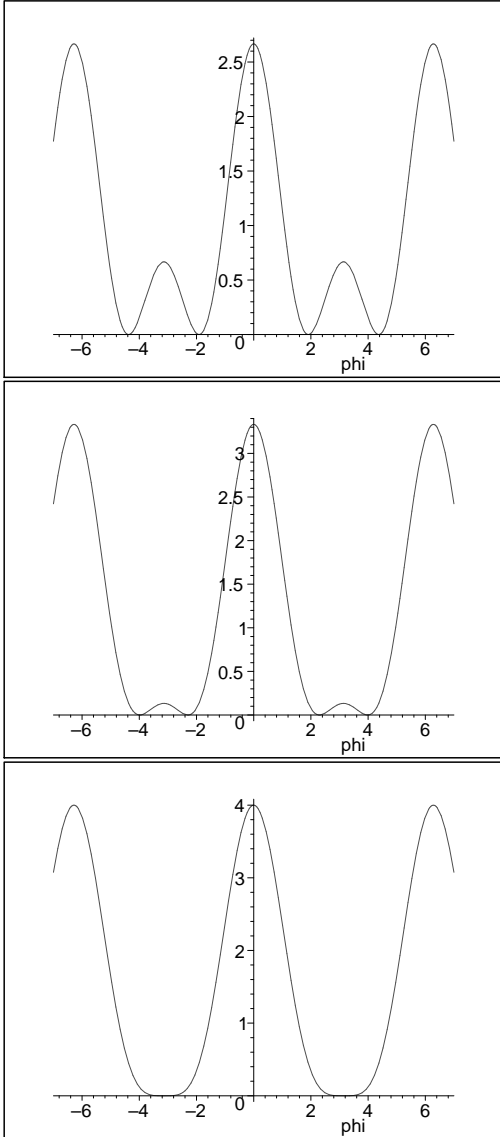


FIG. 1. The double sine-Gordon potential, depicted for $r = 1/3, 2/3$ and 1 from above to below respectively, to illustrate how the behavior of the model changes with r .

We get a better view of the phase transition in the dou-

ble sine-Gordon model by examining the order parameter $\bar{\phi}(r)$, which is given by $\pm\pi \pm \alpha(r)$ for $0 < r \leq 1$, so it goes continuously to $\pm\pi$ for $r \geq 1$. Also, the (squared) mass of the field can be obtained via the relation

$$V_r''(\bar{\phi}) = W_{\bar{\phi}\bar{\phi}}^2 + W_{\bar{\phi}} W_{\bar{\phi}\bar{\phi}\bar{\phi}} \quad (12)$$

where $\bar{\phi}$ is the corresponding minimum of the potential. For $0 < r \leq 1$ we get $m^2(r) = 4 - 4r$, and for $r \geq 1$ we have $m^2(r) = 4(r - 1)/(r + 1)$. We see that $m(r)$ vanishes in the limit $r \rightarrow 1$. These results indicate that r drives a second order phase transition, a transition where the system goes from the case of two distinct phases to another one, engendering a single phase.

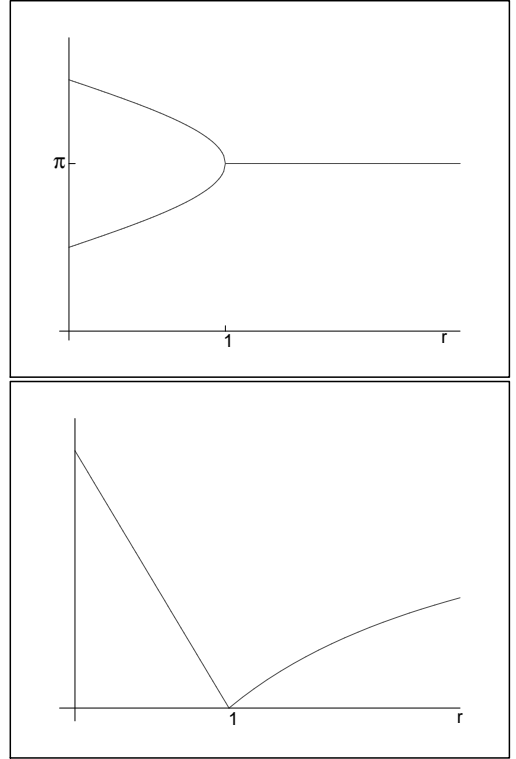


FIG. 2. Plots of $\bar{\phi}(r)$ (above) and $m^2(r)$ (below) for the double sine-Gordon potential, which illustrate how the behavior of the model changes with r .

We consider $0 < r \leq 1$. The energies of the BPS solutions are given as follows. For solutions connecting the minima $-\pi + \alpha(r)$ and $\pi - \alpha(r)$ the defect is large since it joins minima separated by a higher and wider barrier. We have

$$t_{dsG}^l = 4\sqrt{1-r} + 4r \frac{\pi - \alpha(r)}{\sqrt{1+r}} \quad (13)$$

In the case of the minima $\pi - \alpha(r)$ and $\pi + \alpha(r)$ the defect is small and we get

$$t_{dsG}^s = 4\sqrt{1-r} - 4r \frac{\alpha(r)}{\sqrt{1+r}} \quad (14)$$

We notice that $t_{dsG}^l = t_{dsG}^s + 4\pi r/\sqrt{1+r}$, and that the limit $r \rightarrow 1$ sends $t_{dsG}^l \rightarrow 2\sqrt{2}\pi$ and $t_{dsG}^s \rightarrow 0$, as expected. For the BPS states we can write the solutions explicitly. For instance, for solutions that connect the minima $-\pi + \alpha(r)$ and $\pi - \alpha(r)$ we get large kink solutions, which are of the form

$$\phi_l(x) = \pm 2 \tan^{-1} \left[\sqrt{\frac{1+r}{1-r}} \tanh(\sqrt{1-r} x) \right] \quad (15)$$

For solutions that connect the minima $\pi \pm \alpha(r)$ and the minima $-\pi \pm \alpha(r)$ we get small kink solutions. They are given by

$$\phi_s(x) = \pm \pi - 2 \tan^{-1} \left[\sqrt{\frac{1-r}{1+r}} \tanh(\sqrt{1-r} x) \right] \quad (16)$$

The case $r > 1$ is different. The minima are now at $\pm\pi$, and the model is similar to the standard sine-Gordon model. In this case we modify the potential of Eq. (10) to

$$V(\phi) = \frac{2}{r+1} (\cos^2(\phi) + 2r \cos(\phi) + 2r - 1) \quad (17)$$

to make $V(\pm\pi) = 0$. Thus, we can write this potential in terms of another superpotential, such that

$$\widetilde{W}_\phi = \frac{2}{\sqrt{r+1}} \sqrt{\cos^2(\phi) + 2r \cos(\phi) + 2r - 1} \quad (18)$$

The presence of the square root complicates the calculation, and we have been unable to find explicit analytical solutions in this case.

The potential in Eq. (10) in the limit $r \rightarrow 0$ goes to

$$V_0(\phi) = 1 + \cos(2\phi) \quad (19)$$

which leads us back to the sine-Gordon model. Thus, we can suppose r small and use $V_r(\phi)$ to explore the double sine-Gordon model as a model controlled by a small parameter, in the vicinity of the sine-Gordon model. This feature may be of some use for investigations that follow the lines of Ref. [43], and also in the case concerning the presence of internal modes of solitary waves, which seems to appear when one slightly modifies some integrable model – see for instance Ref. [44].

We now turn attention to the third class of models, which is described by two real scalar fields. In this case the domain walls may engender internal structure. This line of investigation follows as in Refs. [11–13] and we illustrate such possibility with the system defined by the potential

$$V(\phi, \chi) = \frac{1}{2}(\phi^1 - 1)^2 + \frac{1}{2}r^2 \left(\chi^2 - \frac{1}{r} \right)^2 + r(1 + 2r)\phi^2\chi^2 \quad (20)$$

where the parameter $r \neq 0$ is real. This model was first investigated in Ref. [45]. This potential follows from the

superpotential $W(\phi, \chi) = \phi - (1/3)\phi^3 - r\phi\chi^2$, and the system supports the two-field solutions $\phi(x) = \tanh(2rx)$ and $\chi(x) = a \operatorname{sech}(2rx)$, with $a^2 = 1/r - 2$. These solutions are BPS solutions, and now the parameter r is restricted to the interval $r \in (0, 1/2)$. The limit $r \rightarrow 1/2$ lead us to the one-field solution $\phi(x) = \tanh(x)$ and $\chi(x) = 0$. The two-field solutions obey $\phi^2 + \chi^2/a^2 = 1$, which describes an elliptic arc connecting the two minima $(\pm 1, 0)$ of the corresponding potential in the (ϕ, χ) plane. The one-field solutions represent standard domain walls, while the two-field solutions may be seen as domain walls having internal structure: the vector (ϕ, χ) in configuration space describes a straight line segment for the one-field solution, and an elliptic arc for the two-field solution, resembling light in the linearly and elliptically polarized cases, respectively. The same solutions appear in condensed matter, in the anisotropic XY model used to describe ferromagnetic transition in magnetic systems, and there they are named Ising and Bloch walls, respectively – see for instance Ref. [3], chapter 7.

In the present work we are especially interested in three other models. They are defined by potentials that describe a single real scalar field

$$V_1(\phi) = \frac{1}{2} - |\phi| + \frac{1}{2}\phi^2 \quad (21)$$

$$V_2(\phi) = \frac{1}{2}\phi^2 - |\phi|\phi^2 + \frac{1}{2}\phi^4 \quad (22)$$

and two real scalar fields

$$V_3(\phi, \chi) = \frac{1}{2}(1 - |\phi|)^2 - r(1 - |\phi|)\chi^2 + \frac{1}{2}r^2\chi^4 + 2r^2\phi^2\chi^2 \quad (23)$$

The first model was investigated in Refs. [46,47] to model an exactly soluble linear chain system. It has also been investigated more recently in Ref. [48] and also in Ref. [43], with different motivations. The other models are new, and some of their classical and quantum features will be examined below.

We notice that the above models can be described by the following superpotentials

$$W_1(\phi) = \phi - \frac{1}{2}|\phi|\phi \quad (24)$$

$$W_2(\phi) = \frac{1}{2}\phi^2 - \frac{1}{3}|\phi|\phi^2 \quad (25)$$

and also

$$W_3(\phi, \chi) = \phi - \frac{1}{2}|\phi|\phi - r\phi\chi^2 \quad (26)$$

The presence of superpotentials help simplifying the investigation, since the BPS solutions satisfy first order differential equations, which are simpler to solve compared to the equations of motion.

Our interest in the first model is directly related to the fact that it is very much similar to the standard ϕ^4

model. Thus, we explore its classical solutions, to see how similar they are to that of the ϕ^4 model. The same for the second model, which was invented to be similar to the ϕ^6 model, and also for the last model, which is an extension of the first model to the case of two fields, in a way similar to the model defined by Eq. (20), as done in Ref. [45].

III. TOPOLOGICAL SOLUTIONS

In this section we search for BPS solutions in the models introduced in the former Sec. II. We investigate the first order equations corresponding to each one of the three models separately.

A. Model 1

This model is defined by the superpotential of Eq. (24). In this case there are two singular points, that represents the two minima of the potential in Eq. (21). These minima are $v_1 = 1, v_2 = -1$. The equation of motion for $\phi = \phi(x)$ is

$$\frac{d^2\phi}{dx^2} = \phi - \frac{\phi}{|\phi|} \quad (27)$$

We are searching for topological solutions, so we can consider instead of the second order differential equation the two first order equations

$$\frac{d\phi}{dx} = \pm(1 - |\phi|) \quad (28)$$

They support the BPS states

$$\phi_{\pm}(x) = \pm 2 \frac{\tanh(x/2)}{1 + \tanh(|x|/2)} \quad (29)$$

After inspecting the explicit form of these BPS solutions, we notice that they have the standard kink-like profile, as in the ϕ^4 model, as we show in Fig. 3. Also, they are linearly stable, minimizing the energy to $t_1 = 1$, below the value $t_s = 4/3$ that appears in the ϕ^4 model.

The interesting feature of this model is that at the classical level it is similar to the ϕ^4 model, although the potential goes up to the second order power in the field. We illustrate the present model and its topological solutions in Fig. 3, where we also plot the topological state of the standard ϕ^4 model to offer a visual comparison between the BPS states of the two models. There we notice that the BPS states of model 1 are thicker than the corresponding states of the ϕ^4 model. Also, we notice that the tension of these BPS states can be written as $t_1 = (3/4)t_s$. This result goes according to conventional wisdom, according to the fact that the energy or tension of kinks and walls in general varies inversely with the width of the defect.

We notice that this model may be used as an alternative to the ϕ^4 model, in applications in condensed matter. For instance, it may represent the motion in the polyacetylene (PA) chain, describing single-double or double-single bound alternation in the PA chain, but this is out of the scope of the present work.

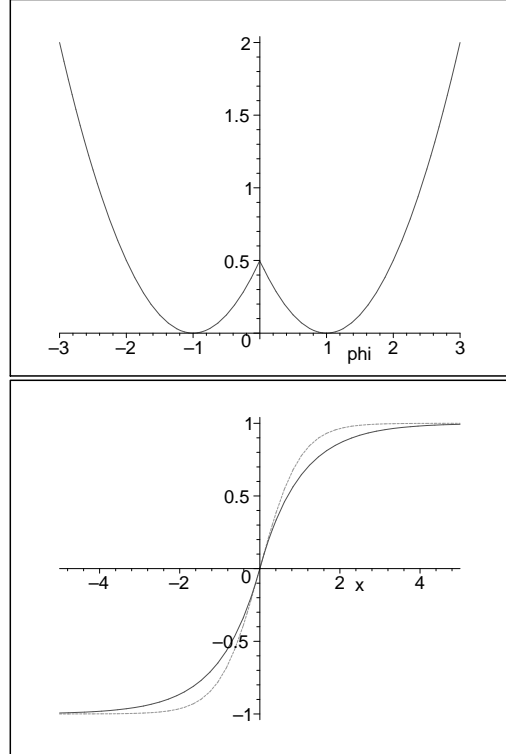


FIG. 3. The potential $V_1(\phi)$ given in Eq.(21), and below the respective topological solution. For comparison, the dotted line shows the topological solution of the ϕ^4 model.

B. Model 2

Now we explore the second model, described by the potential of Eq. (22). It can be written in terms of the superpotential of Eq. (25). This model contains three minima, at the values $v_1 = 1, v_2 = -1, v_3 = 0$. It supports two topological sectors of the BPS type. These sectors are degenerate, and the wall tension is given by $t_2 = 1/6$. The BPS solutions satisfy

$$\frac{d\phi}{dx} = \pm\phi(1 - |\phi|) \quad (30)$$

The solutions are

$$\phi_{\pm}^+(x) = \pm \frac{1}{2} [1 + \tanh(x/2)] \quad (31)$$

$$\phi_{\pm}^-(x) = \pm \frac{1}{2} [1 - \tanh(x/2)] \quad (32)$$

They are similar to the kink solutions that one finds in the ϕ^6 model, as we have shown in Sec. II. We can write

the wall tension in this second model as $t_2 = (2/3)\bar{t}_s$, where \bar{t}_s is the tension value for the BPS solutions of the ϕ^6 model. We illustrate the present model and its topological solutions in Fig. 4. The interesting feature of the second model is that its potential is polynomial, of the fourth order type, but it presents two distinct phases, the asymmetric phase and another one, symmetric, represented by the vanishing minimum, $v_3 = 0$.

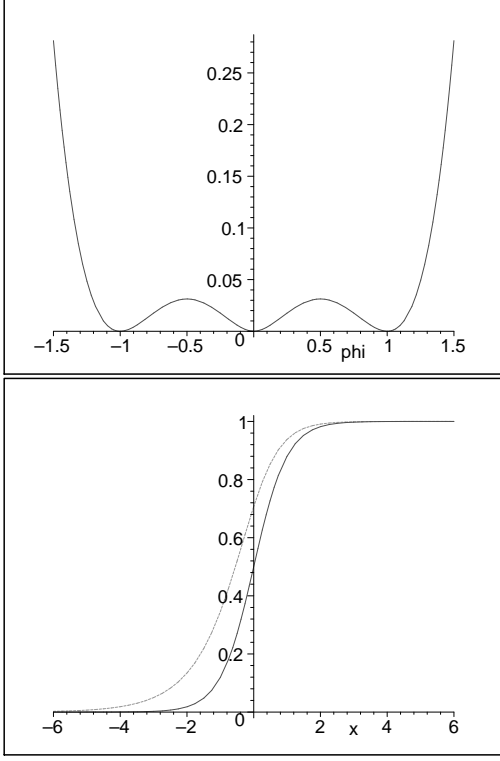


FIG. 4. The potential $V_2(\phi)$ given in Eq.(21), and the respective topological solution. For comparison, the dotted line shows the kink of the ϕ^6 model.

This model seems appropriate to simulate a first order phase transition. However, differently from the ϕ^6 system the present model has the property of having the same squared mass, irrespective of the symmetric or asymmetric phases. To see this we use the potential (22) to obtain

$$\frac{d^2V_2}{d\phi^2} = 1 - 6|\phi| + 6\phi^2 \quad (33)$$

so that $m_2^2(\phi = 0) = m_2^2(\phi = \pm 1) = 1$. As we shall see below, this fact also shows that $U(x) = d^2V_2/d\phi^2$ is symmetric respect to x when calculated at any BPS state, so that the investigation to find the first quantum corrections to the energy of the BPS solutions follows naturally, circumventing the intricacy that happens to appear in the standard ϕ^6 model [42]. The form of the potential of Eq. (22) shows a symmetry respect to $\phi = \pm 1/2$ for ϕ in the interval $0 \leq \phi \leq 1$ – see Fig. 4. This feature does not appear in the ϕ^6 model.

The classical picture that appears for the second model is somehow similar to the picture of the ϕ^6 model. Thus, it may be used as a new model to explore conformational properties of polyethylene (PE), as an alternative to the case investigated in Refs. [35,36]. Moreover, since its potential contains up to the fourth order power in the field, in Sec. V we investigate the semiclassical or one-loop corrections, to see how the thermal effects change the classical picture.

C. Model 3

The third model is given by the potential of Eq. (23). In terms of the superpotential of Eq. (26) the first order equations are

$$\frac{d\phi}{dx} = 1 - |\phi| - r\chi^2 \quad (34)$$

$$\frac{d\chi}{dx} = -2r\phi\chi \quad (35)$$

There are four degenerate minima for $r > 0$, at the points $v_{1,2} = (\pm 1, 0)$ and $v_{3,4} = (0, \pm 1/\sqrt{r})$. There are five BPS sectors, and only one non-BPS sector, which is the sector connecting the minima v_3 and v_4 . The tensions of the BPS states are $t_3^1 = 1$ and $t_3^2 = \sqrt{r}$.

This model is similar to the model considered in Eq. (20). To find BPS solutions we follow Refs. [22,45]. In the sector connecting the minima v_1 and v_2 we have

$$\phi_{\pm}(x) = \pm 2 \frac{\tanh(x/2)}{1 + \tanh(|x|/2)}, \quad \chi(x) = 0 \quad (36)$$

The corresponding orbit is a straight line segment joining the minima v_1 and v_2 . We have been unable to find non trivial BPS states in this sector, for solutions describing an elliptic orbit, although they appear in the model of Eq. (20).

There are other BPS states, in the sectors that connect the minimum v_1 or v_2 to v_3 or v_4 . There are several cases, and we get explicit solutions for the specific value $r = 1/2$, which form straight line segments connecting v_1 or v_2 to v_3 or v_4 . The orbits are described by configurations such that $\chi = \pm\sqrt{2}(\phi \mp 1)$. The explicit solutions are, in the sectors connecting v_2 to v_3 or v_4

$$\phi(x) = -\frac{1}{2}[1 - \tanh(\frac{x}{2})] \quad (37)$$

$$\chi(x) = \pm \frac{\sqrt{2}}{2}[1 + \tanh(\frac{x}{2})] \quad (38)$$

and in the sectors connecting v_1 to v_3 or v_4

$$\phi(x) = \frac{1}{2}[1 + \tanh(\frac{x}{2})] \quad (39)$$

$$\chi(x) = \pm \frac{\sqrt{2}}{2}[1 - \tanh(\frac{x}{2})] \quad (40)$$

These solutions are similar to the solutions found in Ref. [49], for the model of Eq. (20). In Fig. 5 we plot one of the several BPS states that appear in this case.

The nontrivial BPS solutions that we found in model 3 can be used to model domain walls solutions that appear in models for binary mixtures of Bose-Einstein condensates (BEC) [50]. As one knows, for different coupling coefficient between the two BECs, the mixture exhibit complex spatial structure which may be described by domain walls [51]. More importantly, in Ref. [52] one has realized that these domain walls consist of multicomponent solitons. And these multicomponent walls are very much similar to the two-field solutions that we have just found in model 3. A specific feature of the BPS state shown in Fig. 5 is that the limit $x \rightarrow 0$ gives $\phi(0) > \chi(0)$, leading to unequal components in the binary mixture. We shall further explore this issue elsewhere.

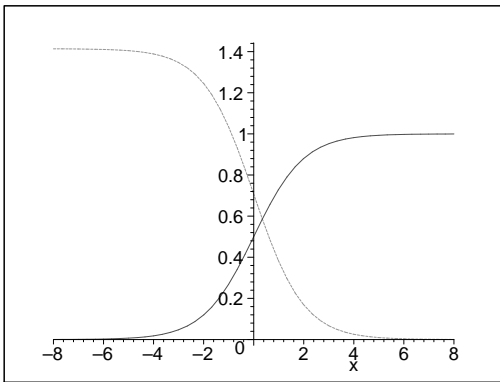


FIG. 5. A typical solution that appear from Eqs. (39) and (40), illustrating how the fields behave as a nontrivial BPS state.

IV. STABILITY

We investigate linear stability of the BPS solutions obtained in the former Sec. III. In the case of a single field the investigation requires that one uses

$$\phi(x, t) = \phi_s(x) + \sum_n \eta_n(x) \cos(w_n t). \quad (41)$$

where $\phi_s(x)$ stands for the static field, and the remaining terms represent the fluctuations about it. Linear stability implies that the fluctuations remains limited in time, so that the set of frequencies $\{w_n\}$ forms a set of real numbers.

We use Eq. (41) into the second order equation of motion (2) to obtain the Schrödinger-like equation $H\eta_n(x) = w_n^2 \eta_n(x)$, where

$$H = -\frac{d^2}{dx^2} + U(x) \quad (42)$$

and

$$U(x) = W_{\phi\phi}^2 - W_{\phi}W_{\phi\phi\phi}. \quad (43)$$

which must be calculated with the static configuration, the BPS states.

As we know, we end up with a supersymmetric quantum mechanical problem. Thus, we generalize the above situation by introducing the pair of Hamiltonians

$$H_{\pm} = -\frac{d^2}{dx^2} + U_{\pm}(x) \quad (44)$$

where

$$U_{\pm}(x) = W_{\phi\phi}^2 \mp W_{\phi}W_{\phi\phi\phi}. \quad (45)$$

These Hamiltonians can be factorized as

$$H_{\pm} = A_{\pm}^{\dagger} A_{\pm} \quad (46)$$

where A_{\pm} are first order operators, given by

$$A_{\pm} = -\frac{d}{dx} \pm W_{\phi\phi} \quad (47)$$

This factorization ensures that the Hamiltonians H_{\pm} are positive definite, so that their eigenvalues are all non-negative real numbers, thus ensuring linear stability of the classical topological solutions.

A. Linear stability: model 1

In order to investigate linear stability of the BPS states obtained in the former Sec. III A, we use Eqs. (2), (29), and (41) to obtain the Schrödinger-like equation

$$\left(-\frac{d^2}{dx^2} + 1 - 2\delta(x)\right) \eta_n(x) = w_n^2 \eta_n(x) \quad (48)$$

In this case the potential is given by

$$U(x) = 1 - 2\delta(x) \quad (49)$$

Stability of the classical solution (29) implies that the eigenvalues of the above Schrödinger-like Eq. (48) should be non-negative. But this is indeed the case, because the attractive potential $\delta(x)$ has only one bound state, and the specific form of the potential $U(x) = 1 - 2\delta(x)$ places this bound state at zero energy. To see this explicitly we follow the steps already presented and we factorize the Hamiltonian in the form

$$-\frac{d^2}{dx^2} + 1 - 2\delta(x) = \left(-\frac{d}{dx} + \frac{|x|}{x}\right) \left(\frac{d}{dx} + \frac{|x|}{x}\right) \quad (50)$$

The single bound state is the zero mode, $\eta_0(x)$, which obeys

$$\left(\frac{d}{dx} + \frac{|x|}{x}\right) \eta_0(x) = 0 \quad (51)$$

This equation is easily solved to give the normalized zero mode

$$\eta_0(x) = e^{-|x|} \quad (52)$$

The quantum mechanical problem is implemented with the partner Hamiltonians. They are

$$H_{\pm} = -\frac{d^2}{dx^2} + U_{\pm}(x) \quad (53)$$

where $U_{\pm}(x) = 1 \pm 2\delta(x)$. They are obtained via $H_{\pm} = A_{\pm}^{\dagger}A_{\pm}$, with the first order differential operators

$$A_{\pm} = \pm \frac{d}{dx} + \frac{|x|}{x} \quad (54)$$

The bosonic model under investigation can be seen as the bosonic portion of a more general theory, which includes fermions via the standard Yukawa coupling. In the model with fermions we can search for fermionic zero modes. The investigation may follow the lines of Ref. [53].

B. Linear stability: model 2

We follow the same steps to investigate stability of the BPS solutions of the second model, given by Eqs. (31) and (32). In this case the Schrödinger-like equation becomes

$$\left(-\frac{d^2}{dx^2} + 1 - \frac{3}{2} \operatorname{sech}^2\left(\frac{x}{2}\right)\right) \eta_n(x) = w_n^2 \eta_n(x) \quad (55)$$

This new Hamiltonian can be factorized as

$$\left(\frac{d}{dx} - \tanh\left(\frac{x}{2}\right)\right) \left(-\frac{d}{dx} - \tanh\left(\frac{x}{2}\right)\right) \quad (56)$$

The zero mode obeys

$$\left(-\frac{d}{dx} - \tanh\left(\frac{x}{2}\right)\right) \eta_0(x) = 0 \quad (57)$$

This first order equation can be integrated easily; the normalized zero mode has the explicit form

$$\eta_0(x) = \frac{1}{2} \sqrt{\frac{3}{2}} \operatorname{sech}^2\left(\frac{x}{2}\right) \quad (58)$$

We notice that the above Schrödinger-like Eq. (55) is the equation that appears in the modified Poschl-Teller problem, so that the investigation here goes very much like it does in the standard ϕ^4 model – see for instance Ref. [4]. As a result, besides the above zero mode the present problem has another bound state, at energy $w_1 = \sqrt{3}/2$ – recall that we are using dimensionless units in the present work. Also, the continuum starts at energy $w = 1$.

The quantum mechanical problem is implemented by the partner Hamiltonians $H_{\pm} = A_{\pm}^{\dagger}A_{\pm}$, where the first order differential operators have the explicit form

$$A_{\pm} = \pm \frac{d}{dx} - \tanh\left(\frac{x}{2}\right) \quad (59)$$

C. Linear stability: model 3

We now direct our attention to the third model. We consider the classical solution (36). In this case we consider $\phi(x, t)$ as before, and $\chi(x, t)$ in the form

$$\chi(x, t) = \sum_n \xi_n(x) \cos(\overline{w}_n t) \quad (60)$$

The Schrödinger-like equation splits into two equations, one of them being exactly Eq. (48), and the other is

$$\left(-\frac{d^2}{dx^2} + U(x)\right) \xi_n(x) = \overline{w}_n^2 \xi_n(x) \quad (61)$$

where

$$U(x) = 2r \frac{8r - (8r + 1) \operatorname{sech}^2(x/2)}{[1 + \tanh(|x|/2)]^2} \quad (62)$$

In this case the potential has at least one bound state, the zero mode. From the analytical point of view the problem is somehow complicated, and we could not find any explicit solutions. However, we could verify that the number of bound states depends on r , and increases for increasing r . As we can see from Eq. (26), the parameter r is related to the way the two fields interact. Thus, one sees that the number of bound states increases when one increases the strength of the interaction between the two fields. This feature also appears in other models, and we shall further explore this specific issue in another work.

V. THERMAL EFFECTS

Let us now deal with semiclassical effects. However, instead of calculating the quantum corrections to the energy of the classical solutions let us investigate the effective potential in the case of a single real scalar field. There are several distinct but equivalent ways of implementing the calculations and we choose to follow Refs. [54,55]. We get the general expression, which is valid at the one-loop level [54]

$$V^1(\phi) = \frac{1}{2} \int \frac{d^4 k}{(2\pi)^4} \ln[k^2 + V''(\phi)] \quad (63)$$

where $V''(\phi) = d^2 V/d\phi^2$, and the metric is now Euclidian. The thermal effects are obtained after changing the one loop contribution of Eq. (63) to

$$V_{\beta}^1(\phi) = \frac{1}{2} \int \frac{d^3 k}{(2\pi)^3} \sum_{n=-\infty}^{\infty} \ln \left[\left(\frac{2\pi n}{\beta} \right)^2 + \mathbf{k}^2 + V''(\phi) \right] \quad (64)$$

The temperature enters the game as $\beta = 1/T$. We make the sum to obtain the finite temperature contribution [55–57]

$$V_\beta^1(\phi) = \frac{1}{\beta} \int \frac{d^3k}{(2\pi)^3} \ln \left[1 - e^{-\beta \sqrt{k^2 + V''(\phi)}} \right] \quad (65)$$

The temperature dependent contribution can be used to investigate how the thermal effects enter the game.

We investigate the second model at finite temperature. We rewrite the potential of Eq. (22) in the form

$$V_2(\phi) = \frac{1}{2} \phi^2 (m - \lambda |\phi|)^2 \quad (66)$$

Here we have introduced m and λ to parametrize the potential, restoring the standard notation that appears with $\hbar = c = 1$. The parameters m and λ are real, and we consider $m/\lambda > 0$ to allow for spontaneous symmetry breaking. We notice that m has dimension of energy, while λ is dimensionless.

The motivation to study this model is that it has an interesting property, not seen in the ϕ^6 model. The above potential goes up to the fourth order power in the field, and it has minima at the nonzero values $|\bar{\phi}| = m/\lambda$ and at $\phi = 0$; however, the classical masses corresponding to these minima degenerate to the single (squared) value m^2 .

In the high temperature limit ($T \gg m$) the one loop effective potential in this case is well approximated by

$$V_{eff}(\phi) = \frac{1}{2} \phi^2 (m - \lambda |\phi|)^2 + \frac{T^2}{24} V''(\phi) \quad (67)$$

where $V''(\phi) = m^2 - 6m\lambda|\phi| + 6\lambda^2\phi^2$. The effective potential has the minima

$$\bar{\phi}_i = \pm \frac{1}{2} \frac{m}{\lambda} \left(1 \pm \sqrt{1 - \frac{\lambda^2}{m^2} T^2} \right) \quad (68)$$

This result allows introducing the critical temperature $T_c = m/\lambda$, which identifies two distinct behaviors: for T below T_c the effective potential supports four minima, at the above values of $\bar{\phi}_i, i = 1, 2, 3, 4$, but for $T \geq T_c$ there are only two minima, at the values $\bar{\phi}_\pm = \pm m/2\lambda$. This behavior reminds us of the double sine-Gordon model shown in Sec. II, although here the driving parameter is the temperature. The behavior of the effective potential is shown in Fig. 6, where we depict two typical cases, for $T = (4/5)T_c$ and for $T = T_c$.

We notice that the high temperature effects are unable to restore the symmetry, which remains broken for $T \geq T_c = m/\lambda$, which is greater than m in the weak coupling limit that makes our calculations reliable. Although this result goes against conventional wisdom, it has already appeared in other models, as for instance in [55,58] and in references therein.

We investigate the (squared) mass, which can be obtained from the effective potential by the usual procedure. It can be written as

$$m^2(T) = V''(\bar{\phi}) + \frac{1}{24} V''''(\bar{\phi}) T^2 \quad (69)$$

Thus, for temperature lower than T_c the masses at the constant configurations $\bar{\phi}_i$ degenerate to the single value

$$m^2(T) = m^2 - \lambda^2 T^2, \quad T \leq T_c \quad (70)$$

For temperature higher than T_c we get

$$m^2(T) = -\frac{m^2}{2} + \frac{\lambda^2}{2} T^2, \quad T \geq T_c \quad (71)$$

These results show that the effective mass decreases to zero for temperature lower than T_c , and it increases from zero for temperature above T_c . The critical temperature identifies the point where the effective mass vanishes, and for higher temperature there is no symmetry restoration anymore.

In Fig. 7 we depict the minima of the potential, and the squared mass at finite temperature. There we see that $\bar{\phi}(T)$ varies continuously as the temperature crosses the critical value $T_c = m/\lambda$, indicating the presence of a second order phase transition.

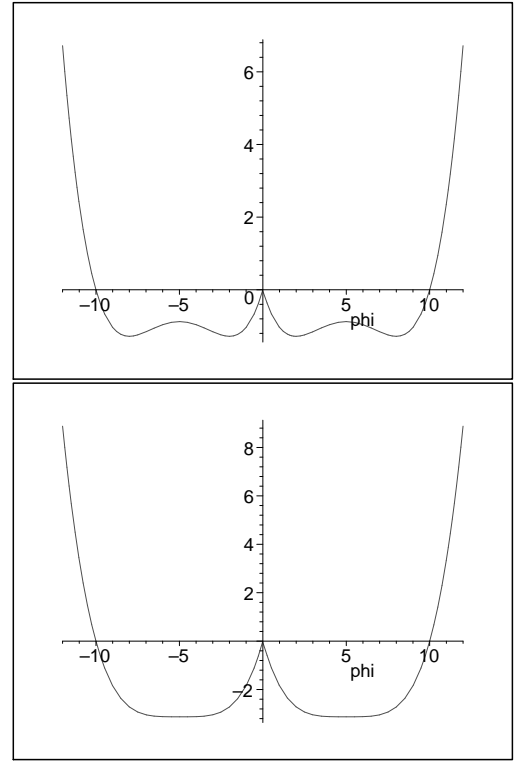


FIG. 6. The effective potential as a function of temperature, for the two typical values $T/T_c = 4/5$ (above) and $T/T_c = 1$ (below).

VI. CONCLUSIONS

In the present work we have investigated several models described by one and by two real scalar fields. The main investigations concern the search for BPS states, that is, for topological solutions that solve first order differential equations. These solutions minimize the energy

to the Bogomol'nyi bound, which is given solely in terms of the superpotential, and the asymptotic value of the corresponding field configurations.

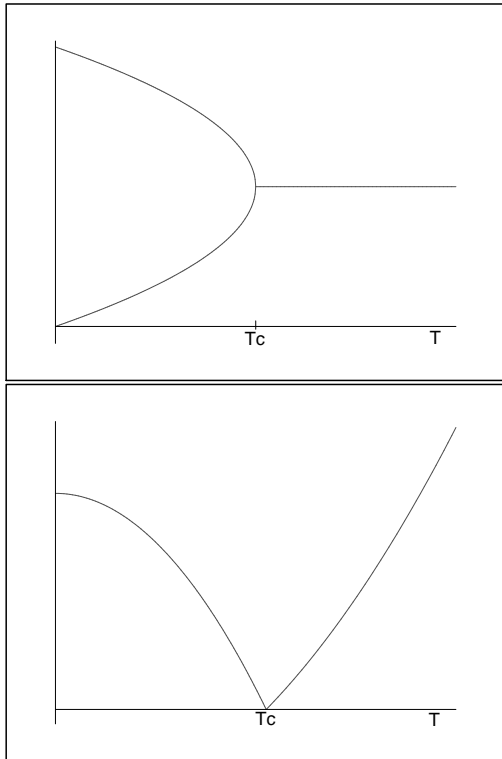


FIG. 7. The minima $\bar{\phi}(T)$ of the effective potential (above), and the effective mass $m^2(T)$ (below), depicted as a function of the temperature.

The search for topological solutions is done at the classical level, and we have paid special attention to models introduced in Sec. II, some of them further explored in Sec. III. These investigations have shown how to write the double sine-Gordon model in terms of a superpotential, and to deal with the large and small kinks as BPS states, as solutions to first order differential equations. We have also shown that model 1 and model 2, defined by the potentials of Eqs. (21) and (22), respectively, are classically similar to the standard field theory models known as the ϕ^4 and the ϕ^6 models. The other model is a two-field model, defined by the potential of Eq. (23). It is similar to a model first investigated in Ref. [45]. The classical investigations that we have developed are of interest in applications to nonlinear science, as for instance in the line of the work presented in Refs. [34–37], where one uses field theory models to mimic nonlinear interactions in polymeric chains. For instance, the model 1 may be used as an alternative to the ϕ^4 model that is standardly considered to mimic the polyacetylene (PA) chain, where Peierls instability appears due to single and double bound alternation in carbon atoms along the chain. The standard scenario leads to the very nice picture in which the distance carbon-carbon

is mapped to the ϕ^4 model with spontaneous symmetry breaking. The need for spontaneous symmetry breaking is to reproduce the two degenerate states, which describe single-double and double-single alternations in the trans or zig-zag PA chain. Of course, this picture can be more interesting if one adds fermions to the system, via the standard Yukawa coupling. The alternative that we propose is to mimic the PA chain with model 1, which is very much similar to the ϕ^4 model at the classical level. We hope to explore this and similar ideas in the near future.

In order to further explore the analogy between standard field theory models and the models here introduced, we have also calculated the thermal effects at the one-loop level. In particular, we have explored the second model, working out the one-loop finite temperature correction to see how the semiclassical contributions may change the classical picture of the model. As we have shown, the finite temperature effects add to the classical potential of model 2 and change it in a way such that it allows for a second order phase transition to take place at high temperature, although the symmetry is never restored by the thermal corrections. The thermal effects in this model 2 remind us of the behavior of the double sine-Gordon model with the parameter r that we investigated in Sec. II.

The potential of the second model is polynomial, and goes up to the fourth order power in the field. In this sense it reminds us of the ϕ^4 model. However, it admits two degenerate but different phases, the symmetric phase that is governed by the vanishing minimum, and the asymmetric phase which is described by the two non-vanishing minima. In this sense it is similar to the ϕ^6 model. However, at the semiclassical level the thermal corrections change the behavior of the model in a way such that it is very specific, reminding us of neither the ϕ^4 nor the ϕ^6 models anymore.

A direct motivation that follows from the present investigations concerns the inclusion of fermions, to see how the fermions change the scenario we have just obtained. Another motivation concerns generalization of the field theory models to the case of complex fields, which give rise to models engendering the continuum $U(1)$ symmetry. In this new scenario the models admit the presence of vortices, global and local, depending on the gauging of the global symmetry that appears when one changes the real field to a complex one. These specific issues are presently under investigation, and we hope to report on them in the near future.

We thank P.L. Christiano, J.R.S. Nascimento, and R.F. Ribeiro for discussions, and CAPES, CNPq, PROCAD and PRONEX for financial support.

- [1] A.H. Eschenfelder, *Magnetic Bubble Technology* (Springer-Verlag, Berlin, 1981).
- [2] B.A. Strukov and A.P. Levanyuk, *Ferroelectric Phenomena in Crystals* (Springer-Verlag, Berlin, 1998).
- [3] D. Walgraef, *Spatio-Temporal Pattern Formation* (Springer-Verlag, New York, 1997).
- [4] R. Rajaraman, *Solitons and Instantons* (North-Holland, Amsterdam, 1982).
- [5] E.W. Kolb and M.S. Turner, *The Early Universe* (Addison-Wesley, Redwood/CA, 1990).
- [6] A. Vilenkin and E.P.S. Shellard, *Cosmic Strings and Other Topological Defects* (Cambridge UP, Cambridge/UK, 1994).
- [7] K. Maki and P. Kumar, Phys. Rev. B **14**, 118 (1976).
- [8] K. Maki and P. Kumar, Phys. Rev. B **14**, 3920 (1976).
- [9] H. Dvey-Aharon, T.J. Sluckin, and P.L. Taylor, Phys. Rev. B **21**, 3700 (1980).
- [10] C.A. Condat, R.A. Guyer, and M.D. Miller, Phys. Rev. B **27**, 474 (1983).
- [11] R. MacKenzie, Nucl. Phys. B **303**, 149 (1888).
- [12] J.R. Morris, Phys. Rev. D **52**, 1096 (1995).
- [13] D. Bazeia, R.F. Ribeiro, and M.M. Santos, Phys. Rev. D **54**, 1852 (1996).
- [14] F.A. Brito and D. Bazeia, Phys. Rev. D **56**, 7869 (1997).
- [15] J.D. Edelstein, M.L. Trobo, F. A. Brito, and D. Bazeia, Phys. Rev. D **57**, 7561 (1998).
- [16] J.R. Morris, Int. J. Mod. Phys. A **13**, 1115 (1998).
- [17] D. Bazeia, H. Boschi-Filho, and F.A. Brito, J. High Energy Phys. **04**, 028 (1999).
- [18] G.W. Gibbons and P.K. Townsend, Phys. Rev. Lett. **83**, 1727 (1999).
- [19] P.M. Saffin, Phys. Rev. Lett. **83**, 4249 (1999).
- [20] H. Oda, K. Naganuma, and N. Sakai, Phys. Lett. B **471**, 148 (1999).
- [21] D. Bazeia and F.A. Brito, Phys. Rev. Lett. **84**, 1094 (2000).
- [22] D. Bazeia and F.A. Brito, Phys. Rev. D **61**, 105019 (2000).
- [23] M. Shifman and T. ter Veldhuis, Phys. Rev. D **62**, 065004 (2000).
- [24] A. Alonso Izquierdo, M.A. Gonzalez Leon, and J. Mateos Guilarte, Phys. Lett. B **480**, 373 (2000).
- [25] R. Hofmann, Phys. Rev. D **62**, 065012 (2000).
- [26] D. Bazeia and F.A. Brito, Phys. Rev. D **62**, 101701(R) (2000).
- [27] D. Binosi and T. ter Veldhuis, Phys. Rev. D **63**, 085016 (2001).
- [28] F.A. Brito and D. Bazeia, Phys. Rev. D **64**, 065022 (2001).
- [29] M. Naganuma and M. Nitta, Prog. Theor. Phys. **105**, 501 (2001).
- [30] M. Naganuma, M. Nitta, and N. Sakai, BPS walls and junctions in SUSY nonlinear sigma models, hep-th/0108179.
- [31] J.H. Schwartz, Nucl. Phys. B (Proc. Suppl.) **55**, 1 (1997).
- [32] J. Maldacena, Adv. Theor. Math. Phys. **2**, 231 (1998).
- [33] A. Giveon and D. Kutasov, Rev. Mod. Phys. **71**, 983 (1999).
- [34] D. Bazeia, R.F. Ribeiro, and M.M. Santos, Phys. Rev. E **54**, 2943 (1996).
- [35] D. Bazeia and E. Ventura, Chem. Phys. Lett. **303**, 341 (1999).
- [36] E. Ventura, A.M. Simas, and D. Bazeia, Chem. Phys. Lett. **320**, 587 (2000).
- [37] D. Bazeia, V.B.P. Leite, B.H.B. Lima, and F. Moraes, Chem. Phys. Lett. **340**, 205 (2001).
- [38] E. B. Bogomol'nyi, Sov. J. Nucl. Phys. **24**, 449 (1976).
- [39] M. K. Prasad and C. M. Sommerfield, Phys. Rev. Lett. **35**, 760 (1975).
- [40] D. Bazeia, J. Menezes, and M.M. Santos, preprint hep-th/0103041.
- [41] D. Bazeia, J. Menezes, and M.M. Santos, preprint hep-th/0110111, Phys. Lett. B, in press.
- [42] M.A. Lohe, Phys. Rev. D **20**, 3120 (1979).
- [43] C.A.G. Almeida, D. Bazeia, and L. Losano, J. Phys. A **34**, 3351 (2001).
- [44] Y.S. Kivshar, D.E. Pelinovsky, T. Cretegny, and M. Peyrard, Phys. Rev. Lett. **80**, 5032 (1998).
- [45] D. Bazeia, M.J. dos Santos, and R.F. Ribeiro, Phys. Lett. A **208**, 84 (1995).
- [46] B. Horowitz, J.A. Krumhansl, and E. Domany, Phys. Rev. Lett. **14**, 778 (1977).
- [47] S.E. Trullinger and R.M. DeLeonardis, Phys. Rev. A **20**, 2225 (1979).
- [48] S. Theodorakis, Phys. Rev. D **60**, 125004 (1999).
- [49] M.A. Shifman and M.B. Voloshin, Phys. Rev. D **57**, 2590 (1998).
- [50] C.J. Myatt *et al.*, Phys. Rev. Lett. **78**, 586 (1997).
- [51] E. Timmermans, Phys. Rev. Lett. **81**, 5718 (1998).
- [52] S. Coen and M. Haelterman, Phys. Rev. Lett. **87**, 140401 (2001).
- [53] D. Bazeia, Phys. Rev. D **60**, 067705 (1999).
- [54] R. Jackiw, Phys. Rev. D **9**, 1686 (1974).
- [55] L. Dolan and R. Jackiw, Phys. Rev. D **9**, 3320 (1974).
- [56] D. Bazeia, G.C. Marques, and I. Ventura, Rev. Bras. Fis. **13**, 253 (1983).
- [57] C. Aragão de Carvalho *et al.*, Phys. Rev. D **31**, 1411 (1985).
- [58] R.N. Mohapatra and G. Senjanović, Phys. Rev. D **20**, 3390 (1979).